

The missing link: discerning true from false negatives when sampling species interaction networks

Michael D. Catchen^{1,2} Timothée Poisot^{3,2} Laura J. Pollock^{1,2} Andrew Gonzalez^{1,2}

¹ McGill University ² Québec Centre for Biodiversity Science ³ Université de Montréal

Correspondance to:

Michael D. Catchen — michael.catchen@mcgill.ca

Abstract: Ecosystems are composed of networks of interacting species. These interactions allow communities of species to persist through time through both neutral and adaptive processes. Despite their importance, a robust understanding of (and ability to predict and forecast) interactions among species remains elusive. This knowledge-gap is largely driven by a shortfall of data—although species occurrence data has rapidly increased in the last decade, species interaction data has not kept pace, largely due to the effort required to sample interactions. This means there are many interactions between species that occur in nature, but we do not know these interactions occur because we have never observed them. These so-called “false-negatives” bias data and hinder inference about the structure and dynamics of interaction networks. Here, we demonstrate the realized rate of false-negatives in data can be quite high, even in thoroughly sampled systems, due to the intrinsic variation in abundances across species in a community. We illustrate how a null model of occurrence detection can be used to estimate the false-negative rate in a given dataset. We also show how to directly incorporate uncertainty due to observation error into model-based predictions of interaction probabilities between species. One hypothesis is that interactions between “rare” species are themselves rare because these species are less likely to encounter one-another than species of higher relative abundance, and that this can (in part) explain the common pattern of nestedness in bipartite interaction networks. However, we demonstrate that across several datasets of spatial or temporally replicated networks, there are positive associations between species co-occurrence and interactions, which suggests these interactions among “rare” species actually exist but simply are not observed. Finally, we assess how false negatives influence various models of network prediction, and recommend directly accounting for observation error in predictive models. We conclude by discussing how the understanding of false-negatives can inform how we design monitoring schemes for species interactions.

1 Introduction

2 Species interactions drive many processes in evolution and ecology. A better understanding of species
3 interactions is an imperative to understand the evolution of life on Earth, to mitigate the impacts of
4 anthropogenic change on biodiversity (Makiola *et al.* 2020), and for predicting zoonotic spillover of
5 disease to prevent future pandemics (Becker *et al.* 2021). At the moment we lack sufficient data to meet
6 these challenges (Poisot *et al.* 2021), largely because species interactions are hard to sample (Jordano
7 2016). Over the past few decades biodiversity data has become increasingly available through remotely
8 collected data and adoption of open data practices (Kenall *et al.* 2014; Stephenson 2020). Still, interaction
9 data remains relatively scarce because sampling typically requires human observation. This induces a
10 constraint on the amount, spatial scale, and temporal frequency of resulting data that it is feasible to
11 collect by humans. Many crowdsourced methods for biodiversity data aggregation (e.g. GBIF, eBird) still
12 rely on automated identification of species, which does not easily generalize to interaction sampling.
13 There is interest in using remote methods for interaction sampling, which primarily detect co-occurrence
14 and derive properties like species avoidance from this data (Niedballa *et al.* 2019). However, co-occurrence
15 itself is not necessarily indicative of an interaction (Blanchet *et al.* 2020). This is an example of semantic
16 confusion around the word “interaction”—for example one might consider competition a type of species
17 interaction, even though it is marked by a lack of co-occurrence between species, unlike other types of
18 interactions, like predation or parasitism, which require both species to be together at the same place and
19 time. Here we consider interaction in the latter sense, where two species have fitness consequences on
20 one-another if (and only if) they are in the sample place at the same time. In addition, here we only
21 consider direct (not higher-order) interactions.

22 We cannot feasibly observe all (or even most) of the interactions that occur in an ecosystem. This means
23 we can be confident two species actually interact if we have a record of it (assuming they are correctly
24 identified), but not at all confident that a pair of species *do not* interact if we have *no record* of those
25 species observed together. In other words, it is difficult to distinguish *true-negatives* (two species never
26 interact) from *false-negatives* (two species interact sometimes, but we do not have a record of this
27 interaction). For a concrete example of a false-negative in a food web, see fig. 1. Because even the most
28 highly sampled systems will still contain false-negatives, there is increasing interest in combining
29 species-level data (e.g. traits, abundance, range, phylogenetic relatedness, etc.) to build models to predict

interactions between species we haven't observed together before (Strydom *et al.* 2021). However, the noise of false-negatives could impact the efficacy of our predictive models and have practical consequences for answering questions about interactions (de Aguiar *et al.* 2019). This data constraint is amplified as the interaction data we have is geographically biased toward the usual suspects (Poisot *et al.* 2021). We therefore need a statistical approach to assessing these biases in the observation process and their consequences for our understanding of interaction networks.

The importance of *sampling effort* and its impact on resulting ecological data has produced a rich body of literature. The recorded number of species in a dataset or sample depends on the total number of observations (Walther *et al.* 1995; Willott 2001), as do estimates of population abundance (Griffiths 1998). This relationship between sampling effort, spatial coverage, and species detectability has motivated more quantitatively robust approaches to account for error in sampling data in many contexts: to determine if a given species is extinct (Boakes *et al.* 2015), to determine sampling design (Moore & McCarthy 2016), and to measure species richness across large scales (Carlson *et al.* 2020). In the context of interactions, an initial concern was the compounding effects of limited sampling effort combined with the amalgamation of data (across both study sites, time of year, and taxonomic scales) could lead any empirical set of observations to inadequately reflect the reality of how species interact (Paine 1988) or the structure of the network as a whole (Martinez *et al.* 1999; McLeod *et al.* 2021). Martinez *et al.* (1999) showed that in a plant-endophyte trophic network, network connectance is robust to sampling effort, but this was done in the context of a system for which observation of 62,000 total interactions derived from 164,000 plant-stems was feasible. In some systems (e.g. megafauna food-webs) this many observations is either impractical or infeasible due to the absolute abundance of the species in question.

The intrinsic properties of ecological communities create several challenges for sampling: first, species are not observed with equal probability—we are much more likely to observe a species of high abundance than one of very low abundance (Poisot *et al.* 2015). Canard *et al.* (2012) presents a null model of food-web structure where species encounter one-another in proportion to each species' relative-abundance. This assumes that there are no associations in species co-occurrence due to an interaction (perhaps because this interaction is “important” for both species; Cazelles *et al.* (2016)), but in this paper we later show increasing strength of these associations leads to increasing probability of false-negatives in interaction data, and that these positive associations are common in existing network data. Second, observed co-occurrence is often equated with meaningful interaction strength, but this is not necessarily the case

60 (Blanchet *et al.* 2020)—a true “non-interaction” would require that neither of two species, regardless of
61 whether they co-occur, ever exhibit any meaningful effect on the fitness of the other. So, although
62 co-occurrence is not directly indicative of an interaction, it is a precondition for an interaction.

63 Here, we illustrate how our confidence that a pair of species never interacts highly depends on sampling
64 effort. We demonstrate how the realized false-negative-rate of interactions is related to the relative
65 abundance of the species pool, and introduce a method to produce a null estimate of the false-negative-rate
66 given total sampling effort (the total count of all interactions seen among all species-pairs) and a method
67 for including uncertainty into model predictions of interaction probabilities to account for observation
68 error. We then confront these models with data, by showing that positive associations in co-occurrence
69 data can increase the realized number of false-negatives and by showing these positive associations are
70 rampant in network datasets. We conclude by recommending that the simulation of sampling effort and
71 species occurrence can and should be used to help design surveys of species interaction diversity (Moore &
72 McCarthy 2016), and by advocating use of null models like those presented here as a tool for both guiding
73 design of surveys of species interactions and for including detection error into predictive models.

74 **Accounting for false-negatives in species interactions**

75 In this section, we demonstrate how differences in species’ relative-abundance can lead to many
76 false-negatives in interaction data. We also introduce a method for producing a null estimate of the
77 false-negative-rate in datasets via simulation. Because the true false-negative-rate is latent, we can never
78 actually be sure how many false-negatives are in our data. However, here we outline an approach to deal
79 with this fact—first by using simulation to estimate the false-negative-rate for a dataset of a fixed size
80 using neutral models of observation. We then illustrate how to incorporate uncertainty directly into
81 predictions of species interactions to account for observation error based on null estimates of both
82 false-positive rates (as an priori estimate of species misidentification probability) and false-positive rates
83 (as generated via the method we introduce).

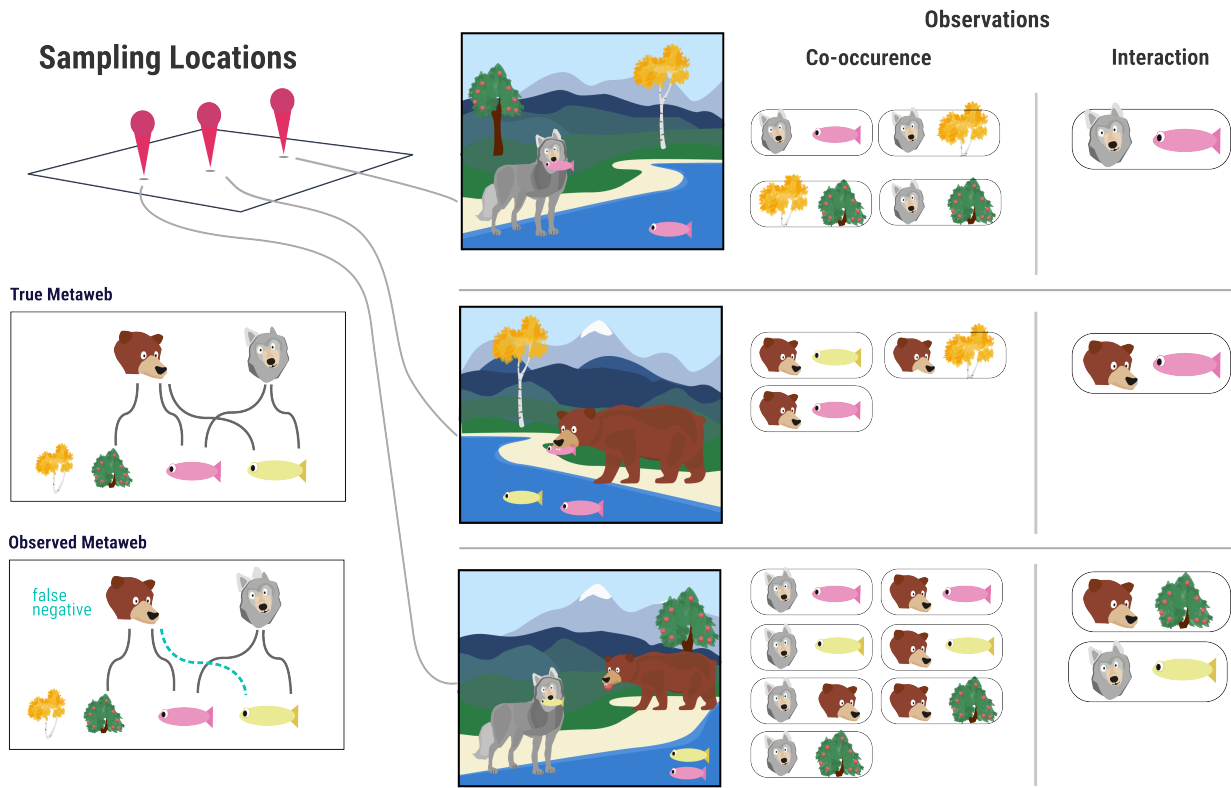


Figure 1: This conceptual example considers a sample of the trophic community of bears, wolves, salmon (pink fish), pike (yellow fish), berry trees, and aspen trees. The true metaweb (all realized interactions across the entire spatial extent) is shown on the left. In the center is what a hypothetical ecologist samples at each site. Notice that although bears are observed co-occurring with both salmon and pike, there was never a direct observation of bears eating pike, even though they actually do. Therefore, this interaction between bears and pike is a false-negative.

How many observations of a non-interaction do we need to be confident it's a true negative?

We start with a naive model of interaction detection: we assume that every interacting pair of species is incorrectly observed as not-interacting with an independent and fixed probability, which we denote p_{fn} and subsequently refer to as the False-Negative-Rate (FNR). If we observe the same species not-interacting N times, then the probability of a true-negative (denoted p_{tn}) is given by $p_{tn} = 1 - (p_{fn})^N$. This relation (the probability-mass-function of geometric distribution, a special case of the negative-binomial distribution) is shown in fig. 2(a) for varying values of p_{fn} and illustrates a fundamental link between our ability to reliably say an interaction doesn't exist— p_{tn} —and the number of times N we have observed a given species. In addition, note that there is no non-zero p_{fn} for which we can ever *prove* that an interaction does not exist—no matter how many observations of non-interactions N we have, $p_{tn} < 1$.

From fig. 2(a) it is clear that the more often we see two species co-occurring, but *not interacting*, the more likely the interaction is a true-negative. This has several practical consequences: first it means negatives taken outside the overlap of the range of each species aren't informative because co-occurrence was not possible, and therefore neither was an interaction. If some of the “worst-case” FNRs presented in fig. 2(a) seem unrealistically high, considering that species are observed in proportion to their relative abundance. In the next section we demonstrate that the distribution of abundance in ecosystems can lead to very high realized values of FNR (p_{fn}) simply as an artifact of sampling effort. Second, we can use this relation to compute the expected number of total observations needed to obtain a “goal” number of observations of a particular pair of species (fig. 2(b)). As an example, if we hypothesize that A and B do not interact, and we want to see species A and B both co-occurring and *not interacting* 10 times to be confident this is a true negative, then we need an expected 1000 observations of all species if the relative abundances of A and B are both 0.1.

False-negatives as a product of relative abundance

We now show that the realized FNR changes drastically with sampling effort due to the intrinsic variation of the abundance of individuals of each species within a community. We do this by simulating the process of observation of species interactions, applied both to 243 empirical food webs from the Mangal database (Banville *et al.* 2021) and random food-webs generated using the niche model, a simple generative model



Figure 2: **(a)** The probability that an observed interaction is a true negative (y-axis) given how many times it has been sampled as a non-interaction (x-axis). Each color reflects a different value of p_{fn} , the false-negative-rate (FNR)—this is effectively the cumulative distribution function (cdf) of the geometric distribution. **(b)** The expected number of total observations needed (colors) to observe 10 co-occurrences between a species with relative abundance $P(A)$ (x-axis) and a second species with relative abundance $P(Y)$. **(c)**: false-negative-rate (y-axis) as a function of total sampling effort (x-axis) and network size, computed using the method described above. For 500 independent draws from the niche model (Williams & Martinez (2000)) at varying levels of species richness (colors) with connectance drawn according to the flexible-links model (MacDonald *et al.* (2020)) as described in the main text. For each draw from the niche model, 200 sets of 1500 observations are simulated, for which the mean false-negative-rate at each observation-step is computed. Means denoted with points, with 1 in the first shade and 2 in the second. **(d)**: Same as **(c)**, except using empirical food webs from Mangal database, where richness. The outlier on **(d)** is a 714 species food-web.

of food-web structure that accounts for allometric scaling (Williams & Martinez 2000). Our neutral model of observation assumes each observed species is drawn in proportion to each species' abundance at that place and time. The abundance distribution of a community can be reasonably-well described by a log-normal distribution (Volkov *et al.* 2003). In addition to the log-normal distribution, we also tested the case where the abundance distribution is derived from power-law scaling $Z^{(\log(T_i)-1)}$ where T_i is the trophic level of species i and Z is a scaling coefficient (Savage *et al.* 2004), which yields the same qualitative behavior. The practical consequence of abundance distributions spanning many orders of magnitude of abundance is that observing two “rare” species interacting requires two low probability events: observing two rare species *at the same time*.

To simulate the process of observation, for an ecological network M with S species, we sample abundances for each species from a standard-log-normal distribution. For each true interaction in the adjacency matrix M (i.e. $M_{ij} = 1$) we estimate the probability of observing both species i and j at a given place and time by simulating n observations of all individuals of any a species, where the species of the individual observed at the $\{1, 2, \dots, n\}$ -th observation is drawn from the generated log-normal distribution of abundances. For each pair of species (i, j) , if both i and j are observed within the n -observations, the interaction is tallied as a true positive if $M_{ij} = 1$. If only one of i or j are observed—but not both—in these n observations, but $M_{ij} = 1$, this is counted as a false-negative, and a true-negative otherwise. For each pair of species (i, j) , if both i and j are observed within the n -observations, the interaction is tallied as a true positive if $M_{ij} = 1$. If only one of i or j are observed—but not both—in these n observations, but $M_{ij} = 1$, this is counted as a false-negative, and a true-negative otherwise ($M_{ij} = 0$). This process is illustrated conceptually in fig. 3(a). In fig. 2(c) we see this model of observation applied to niche model networks across varying levels of species richness, and in fig. 2(d) the observation model applied to Mangal food webs. For all niche model simulations in this manuscript, for a given number of species S the number of interactions is drawn from the flexible-links model fit to Mangal data (MacDonald *et al.* 2020), effectively drawing the number of interactions L for a random niche model food-web as

$$L \sim \text{BetaBinomial}(S^2 - S + 1, \mu\phi, 1 - \mu\phi)$$

where the maximum *a posteriori* (MAP) estimate of (μ, ϕ) applied to Mangal data from (MacDonald *et al.* 2020) is $(\mu = 0.086, \phi = 24.3)$. All simulations were done with 500 independent replicates of unique niche

139 model networks per unique number of observations n . All analyses presented here are done in Julia v1.8
140 (Bezanson *et al.* 2015) using both EcologicalNetworks.jl v0.5 and Mangal.jl v0.4 (Banville *et al.* 2021) and
141 are hosted on [Github](#)). Note that the empirical data, for the reasons described above, very likely already
142 contains many false-negatives, we'll revisit this issue in the final section.

143 From fig. 2(c) it is evident that the number of species considered in a study is inseparable from the
144 false-negative-rate in that study, and this effect should be taken into account when designing samples of
145 ecological networks in the future. We see a similar qualitative pattern in fig. 2(d) where the FNR drops off
146 quickly as a function of observation effort, mediated by total richness. The practical consequence of the
147 bottom row of fig. 2 is whether the total number of observations of all species (the x-axis) for the threshold
148 FNR we deem acceptable (the y-axis) is feasible. This raises two points: first, empirical data on
149 interactions are subject to the practical limitations of funding and human-work hours, and therefore
150 existing data tend to fall on the order of hundreds or thousands observations of individuals per site. Clear
151 aggregation of data on sampling effort has proven difficult to find and a meta-analysis of network data and
152 sampling effort seems both pertinent and necessary, in addition to the effects of aggregation of interactions
153 across taxonomic scales (Gauzens *et al.* 2013; Giacomuzzo & Jordán 2021). This inherent limitation on
154 in-situ sampling means we should optimize where we sample across space so that for a given number of
155 samples, we obtain the maximum information possible. Second, what is meant by “acceptable” FNR? This
156 raises the question: does a shifting FNR lead to rapid transitions in our ability inference and predictions
157 about the structure and dynamics of networks, or does it produce a roughly linear decay in model efficacy?
158 We explore this in the next section.

159 We conclude this section by advocating for the use of neutral models similar to above to generate
160 expectations about the number of false-negatives in a data set of a given size. This could prove fruitful
161 both for designing surveys of interactions but also because we may want to incorporate models of
162 imperfect detection error into predictive interactions models, as Joseph (2020) does for species occurrence
163 modeling. Additionally, we emphasize that one must consider the context for sampling—is the goal to
164 detect a particular species (as in fig. 2(c)), or to get a representative sample of interactions across the
165 species pool? These arguments are well-considered when sampling individual species (Willott 2001), but
166 have not yet been adopted for designing samples of communities.

Including observation error in interaction predictions

Here we show how to incorporate uncertainty into model predictions of interaction probability to account for imperfect observation (both false-negatives and false-positives). Models for interaction prediction typically yield a probability of interaction between each pair of species, p_{ij} . When these are considered with uncertainty, it is usually model-uncertainty, e.g. the variance in the interaction probability prediction across several cross-validation folds, where the data is split into training and test sets several times. The method we introduce adjusts the value of a model's predictions to produce a distribution of interaction probabilities, which are adjusted by a given false-negative-rate p_{fn} and false-positive-rate p_{fp} (outlined in figure fig. 3). We describe first how to sample from this distribution of adjusted interaction probabilities via simulation, and show that this distribution can be well-approximated analytically.

We then consider the output prediction from an arbitrary prediction model, which is the probability p_{ij} that two species i and j interact. To get an estimate of p_{ij} that accounts for observation error, we resample the probability of each interaction p_{ij} by simulating a set of several 'particles,' where each particle is a realization of an interaction occurring (either true or false with probabilities p_{ij} and $1 - p_{ij}$ respectively) and then being correctly observed with probabilities given by p_{fp} and p_{fn} to yield a single boolean outcome for each particle ("Resampling" within fig. 3(b)). Across of many particles, the resulting frequency of 'true' outcomes is a single resample of the interaction probability p_{ij}^* . Across several samples each of several particles, this forms a distribution of probabilities which are adjusted by the true and false negative rates.

There is also an analytic way to approximate this distribution using the normal approximation to binomial. As a reminder, as the total number of samples N from a binomial distribution for n trials with success probability p from approaches infinity, the sum of total successes across all samples approaches a normal distribution with mean np and variance $np(1 - p)$. We can use this to correct the estimate p_{ij} based on the expected false-negative-rate p_{fn} and false-positive rate p_{fp} to obtain the limiting distribution as the number of resamples approaches infinity for the resampled p_{ij}^* for a given number of particles n_p . We do this by first adjusting for the rates of observation error to get the mean resampled probability, $\mathbb{E}[p_{ij}^*]$, as

$$\mathbb{E}[p_{ij}^*] = p_{ij}(1 - p_{fp}) + (1 - p_{ij})p_{fn}$$

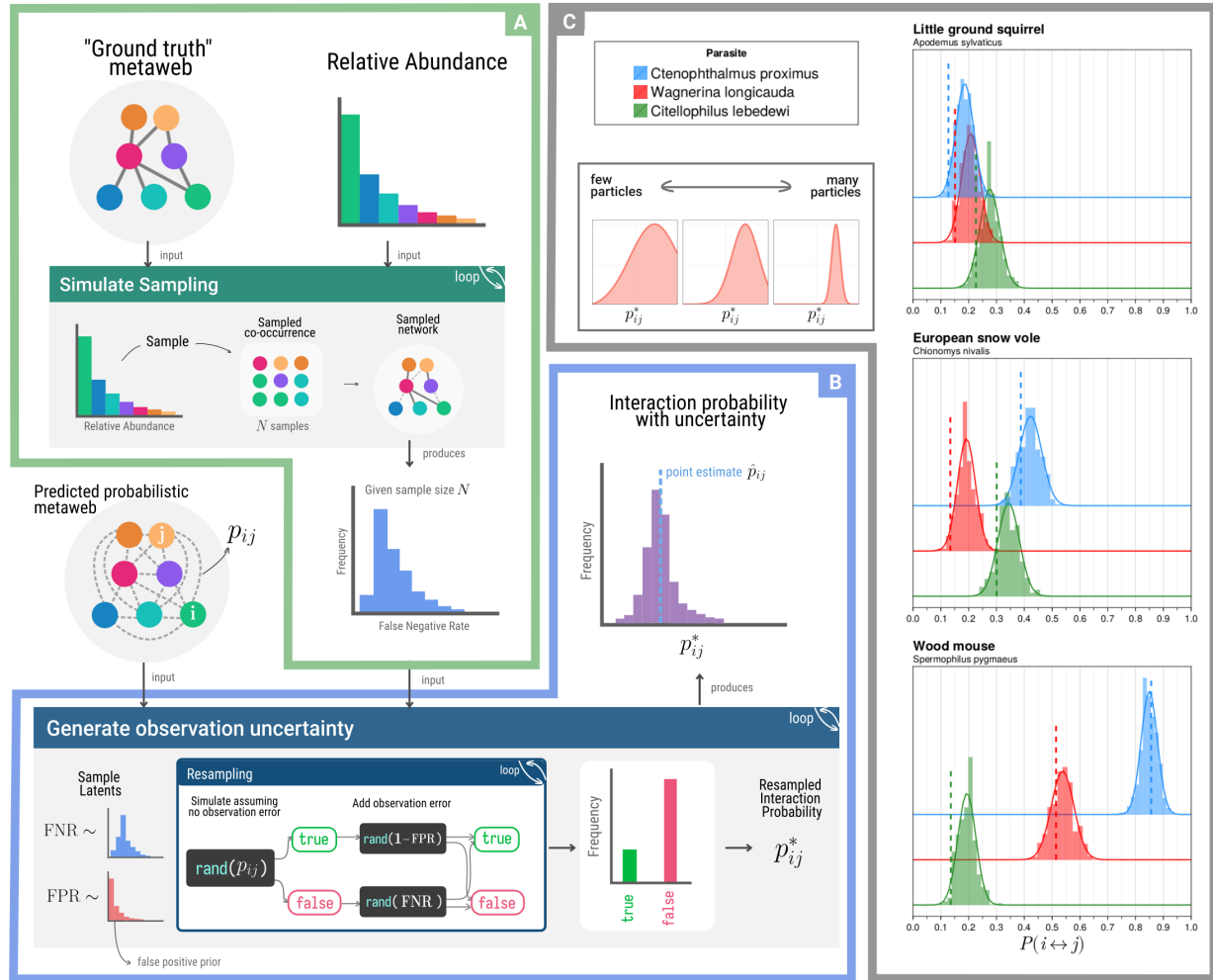


Figure 3: (a) The process for estimating the false-negative-rate (FNR) for an interaction dataset consisting of N total observed interactions. (b) The method for resampling interaction probability based on estimates of false-negative and false-positive rates. (c) The method for interaction probability resampling applied to three mammals and three parasites from the Hadfield *et al.* (2014) dataset. The original probability p_{ij} is indicated with a vertical dashed line. The histogram is simulated from the resampling process, and the line indicates the gaussian approximation to this distribution. Both resampling simulations and the gaussian approximation is applied with $n_p = 150$

193 which is obtainable by definition (supp 1.)

194 For notation, here we refer to a normal distribution with mean μ and standard-deviation σ as $\mathcal{N}(\mu, \sigma)$

195 Then yields the normal approximation

$$\sum_{i=1}^{n_p} p_{ij}^* \sim \mathcal{N}\left(n_p \cdot \mathbb{E}[p_{ij}^*], \sqrt{n_p \mathbb{E}[p_{ij}^*](1 - \mathbb{E}[p_{ij}^*])}\right)$$

196 which then can be converted back to a distribution of frequency of successes to yield the final

197 approximation

$$p_{ij}^* \sim \mathcal{N}\left(\mathbb{E}[p_{ij}^*], \sqrt{\frac{\mathbb{E}[p_{ij}^*](1 - \mathbb{E}[p_{ij}^*])}{n_p}}\right) \quad (1)$$

198 We can then further truncate this distribution to remain on the interval $(0, 1)$, as the output is a
199 probability, although in practice often the probability mass outside $(0, 1)$ is extremely low except for p_{ij}
200 values very close to 0 or 1. As an example case study, we use a boosted-regression-tree to predict
201 interactions in a host-parasite network (Hadfield *et al.* 2014) (with features derived in the same manner as
202 Strydom *et al.* (2021) derives features on this data) to produce a set of interaction predictions. We then
203 applied this method to a set of a few resampled interaction probabilities between mammals and parasite
204 species shown in figure fig. 3(c).

205 Why is this useful? For one, this analytic method avoids the extra computation required by simulating
206 samples from this distribution directly. Further, it enables the extension of the natural analogue between
207 n_p (the number of particles) and the number of observations of co-occurrence for a given pair of
208 species—the fewer the particles, the higher the variance of the resulting approximation. The normal
209 approximation is undefined for 0 particles (i.e. 0 observations co-occurrence), although as n_p approaches 0
210 the approximated normal (once truncated) approaches the uniform distribution on the interval $(0, 1)$, the
211 maximum entropy distribution where we have no information about the possibility of an interaction.

212 This also has implications for what we mean by ‘uncertainty’ in interaction predictions. A model’s
213 prediction can be ‘uncertain’ in two different ways: (1) the model’s predictions may have high variance, or
214 (2) the model’s predictions may be centered around a probability of interaction of 0.5, where we are the
215 most unsure about whether this interaction exists. Improving the incorporation of different forms of

216 uncertainty in probabilistic interaction predictions seems a necessary next step toward understanding
217 what pairs of species we know the least about, in order to prioritize sampling to provide the most new
218 information possible.

219 **Positive associations in co-occurrence increase the false-negative-rate**

220 The model above doesn't consider the possibility that there are positive or negative associations which shift
221 the probability of species cooccurrence away from what is expected based on their relative abundances due
222 to their interaction (Cazelles *et al.* 2016). However, here we demonstrate that the probability of having a
223 false-negative can be higher if there is some positive association in the occurrence of species A and B . If
224 we denote the probability that we observe the co-occurrence of two species A and B as $P(AB)$ and if there
225 is no association between the marginal probabilities of observing A and observing B , denoted $P(A)$ and
226 $P(B)$ respectively, then the probability of observing their co-occurrence is the product of the marginal
227 probabilities for each species, $P(AB) = P(A)P(B)$. In the other case where there is some positive strength
228 of association between observing both A and B because this interaction is "important" for each species,
229 then the probability of observation both A and B , $P(AB)$, is greater than $P(A)P(B)$ as $P(A)$ and $P(B)$ are
230 not independent and instead are positively correlated, i.e. $P(AB) > P(A)P(B)$. In this case, the probability
231 of observing a single false-negative in our naive model from fig. 2(a) is $p_{fn} = 1 - P(AB)$, which due to the
232 above inequality implies $p_{fn} > 1 - P(A)P(B)$. This indicates an increasingly greater probability of a false
233 negative as the strength of association gets stronger, $P(AB) \rightarrow P(AB) \gg P(A)P(B)$. However, this still does
234 not consider variation in species abundance in space and time (Poisot *et al.* 2015). If positive or negative
235 associations between species structure variation in the distribution of $P(AB)$ across space/time, then the
236 spatial/temporal biases induced by data collection would further impact the realized false-negative-rate, as
237 the probability of false negative would not be constant for each pair of species across sites.

238 To test for these positive associations in data we scoured Mangal for datasets with many spatial or temporal
239 replicates of the same system, which led to the resulting seven datasets set in figure fig. 4. For each
240 dataset, we compute the marginal probability $P(A)$ of occurrence of each species A across all networks in
241 the dataset. For each pair of interacting species A and B , we then compute and compare the probability of
242 co-occurrence if each species occurs independently, $P(A)P(B)$, to the empirical joint probability of
243 co-occurrence, $P(AB)$. Following our analysis above, if $P(AB)$ is greater than $P(A)P(B)$, then we expect

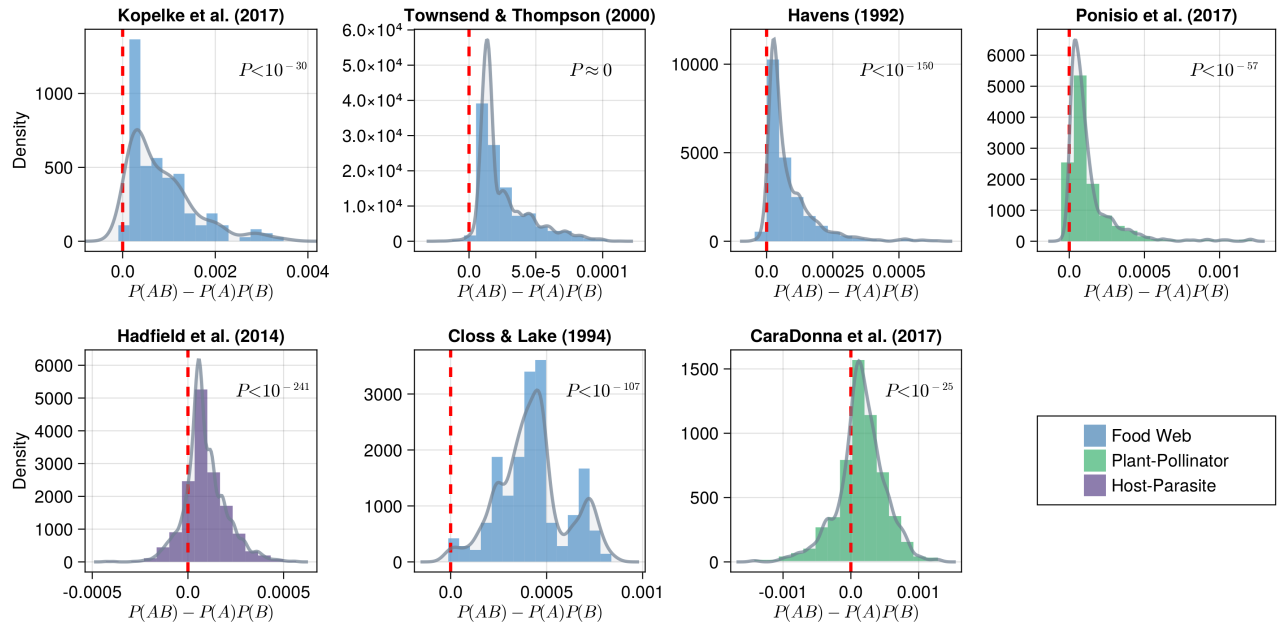


Figure 4: The difference between joint-probability of co-occurrence ($P(AB)$) and expected probability of co-occurrence under independence ($P(A)P(B)$) for interacting species for each dataset. The red-dashed line indicates 0 (no association). Each histogram represents a density, meaning the area of the entire curve sums to 1. The continuous density estimate (computed using local smoothing) is shown in grey. The p-value on each plot is the result of a one-sided t-test comparing the mean of each distribution to 0.

our neutral estimates of the FNR above to underestimate the realized FNR. In fig. 4, we see the difference between $P(AB)$ and $P(A)P(B)$ for the seven suitable datasets with enough spatio-temporal replicates and a shared taxonomic backbone (meaning all individual networks use common species identifiers) found on Mangal to perform this analysis. Further details about each dataset are reported in tbl. 1.

In each of these datasets, the joint probability of co-occurrence $P(AB)$ is decisively greater than our expectation if species co-occur in proportion to their relative abundance $P(A)P(B)$. This suggests that there may not be as many “neutrally forbidden links” (Canard *et al.* 2012) as we might think, and that the reason we do not have records of interactions between rare species is probably due to observation error. This has serious ramifications for the widely observed property of nestedness seen in bipartite networks (Bascompte & Jordano 2007)—perhaps the reason we have lots of observations between generalists is because they are more abundant, and this is particularly relevant as we have strong evidence that generalism drives abundance (Song *et al.* 2022a), not vice-versa.

Table 1: The datasets used in the above analysis (Fig 2). The table reports the type of each dataset, the total number of networks in each dataset (N), the total species richness in each dataset (S), the connectance of each metaweb (all interactions across the entire spatial-temporal extent) (C), the mean species richness across each local network \bar{S} , the mean connectance of each local network \bar{C} , the mean β -diversity among overlapping species across all pairs of network species ($\bar{\beta}_{OS}$), and the mean β -diversity among all species in the metaweb ($\bar{\beta}_{WN}$). Both metrics are computed using KGL β -diversity (Koleff *et al.* 2003)

Network	Type	N	S	C	\bar{S}	\bar{C}	$\bar{\beta}_{OS}$	$\bar{\beta}_{WN}$
Kopelke <i>et al.</i> (2017)	Food Web	100	98	0.037	7.87	0.142	1.383	1.972
Thompson & Townsend (2000)	Food Web	18	566	0.014	80.67	0.049	1.617	1.594
Havens (1992)	Food Web	50	188	0.065	33.58	0.099	1.468	1.881
Ponisio <i>et al.</i> (2017)	Pollinator	100	226	0.079	23.0	0.056	1.436	1.870
Hadfield <i>et al.</i> (2014)	Host-Parasite	51	327	0.085	32.71	0.337	1.477	1.952
Closs & Lake (1994)	Food Web	12	61	0.14	29.09	0.080	1.736	1.864
CaraDonna <i>et al.</i> (2017)	Pollinator	86	122	0.18	21.42	0.312	1.527	1.907

The impact of false-negatives on network properties and prediction

Here, we assess the effect of false-negatives on our ability to make predictions about interactions, as well as their effect on network structure. The prevalence of false-negatives in data is the catalyst for interaction prediction in the first place, and as a result methods have been proposed to counteract this bias (Stock *et al.* 2017; Poisot *et al.* 2022). However, it is feasible that the FNR in a given dataset is so high that it could induce too much noise for an interaction prediction model to detect the signal of possible interaction between species.

To test this we use the dataset from Hadfield *et al.* (2014) that describes host-parasite interaction networks sampled across 51 sites, and the same method as Strydom *et al.* (2021) to extract latent features for each species in this dataset based on applying PCA to the co-occurrence matrix. We then predict a metaweb (equivalent to predicting true or false for an interaction between each species pair, effectively a binary classification problem) from these species-level features using four candidate models for binary classification—three often used machine-learning (ML) methods (Boosted Regression Tree (BRT), Random Forest (RF), Decision Tree (DT)), and one naive model from classic statistics (Logistic Regression (LR)). Each of the ML models are bootstrap aggregated (or bagged) with 100 replicates each. We partition

271 the data into 80-20 training-test split, and then seed the training data with false negatives at varying rates,
272 but crucially do nothing to the test data. We fit all of these models using MLJ.jl, a high-level Julia
273 framework for a wide-variety of ML models (Blaom *et al.* 2020). We evaluate the efficacy of these models
274 using two common measures of binary classifier performance: the area under the receiver-operator curve
275 (ROC-AUC) and the area under the precision-recall curve (PR-AUC), for more details see Poisot (2022).
276 Here, PR-AUC is slightly more relevant as it is a better indicator of prediction of false-negatives. The
277 results of these simulations are shown in fig. 5(a & b).

278 One interesting result seen in fig. 5(a & b) is that the ROC-AUC value does not approach random in the
279 same way the PR-AUC curve does as we increase the added FNR. The reason for this is that ROC-AUC is
280 fundamentally not as useful a metric in assessing predictive capacity as PR-AUC. As we keep adding more
281 false-negatives, the network eventually becomes a zeros matrix, and these models can still learn to predict
282 “no-interaction” for all possible species pairs, which does far better than random guessing (ROC-AUC =
283 0.5) in terms of the false positive rate (one of the components of ROC-AUC). This highlights a more broad
284 issue of label class imbalance, meaning there are far more non-interactions than interactions in data. A
285 full treatment of the importance of class-balance is outside the scope of this paper, but is explored in-depth
286 in Poisot (2022). Further we see, if anything, gradual decline in the performance of the model until we
287 reach very high FNR levels (i.e. $p_{fn} > 0.7$). This is consistent with other recent work (Gupta *et al.* 2023),
288 although it must be considered that the empirical data on which these models are trained already are
289 almost certain to already contain false-negatives.

290 Although these ML models are surprisingly performant at link prediction given their simplicity, there
291 have been several major developments in applying deep-learning methods to many tasks in network
292 inference and prediction—namely graph-representation learning (GRL, Khoshraftar & An (2022)) and
293 graph convolutional networks (Zhang *et al.* 2019). At this time, these advances can not yet be applied to
294 ecological networks because they require far more data than we currently have. We already have lots of
295 features that could be used as inputs into these models (i.e. species level data about occurrence, genomes,
296 abundance, etc.), but our network datasets barely get into the hundreds of local networks sampled across
297 space and time (tbl. 1). Once we start to get into the thousands, these models will become more useful, but
298 this can only be done with systematic monitoring of interactions. This again highlights the need to
299 optimize our sampling effort to maximize the amount of information contained in our data given the
300 expense of sampling interactions.

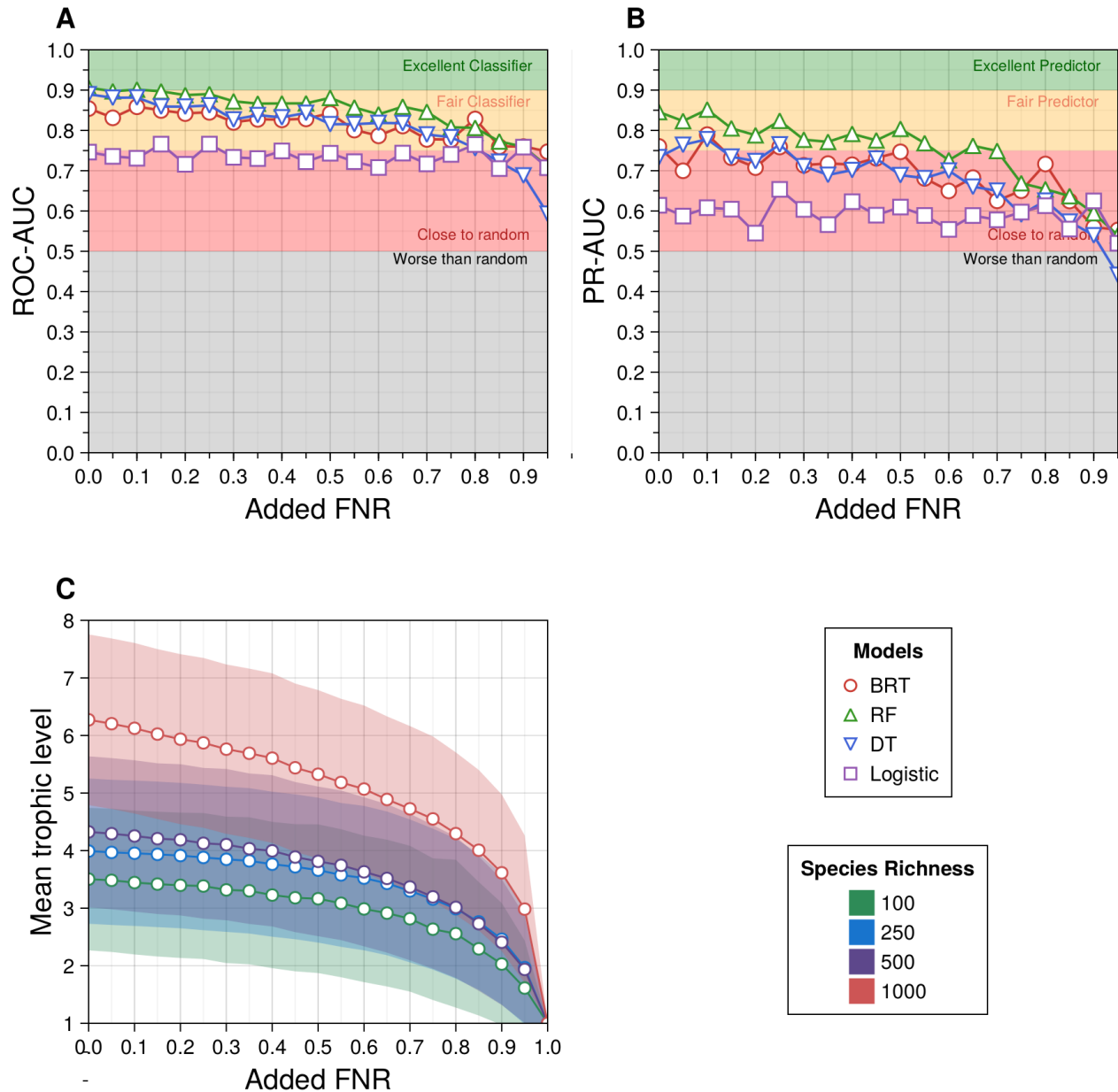


Figure 5: **(a)** The area-under the receiver-operator curve (ROC-AUC) and **(b)** The area-under the precision-recall curve (PR-AUC; right) for each different predictive model (colors/shapes) across a spectrum of the proportion of added false-negatives (x-axis). **(c)** The mean trophic-level of all species in a network generated with the niche model across different species richnesses (colors). For each value of the FNR, the mean trophic level was computed across 50 replicates. The shaded region for each line is one standard-deviation across those replicates.

301 We also consider how the FNR affects network properties. In fig. 5(c) we see the mean trophic level across
302 networks simulated using the niche model (as above), across a spectrum of FNR values. In addition to the
303 clear dependence on richness, we see that mean trophic level, despite varying widely between niche model
304 simulations, tends to be relatively robust to false-negatives and does not deviate widely from the true value
305 until very large FNRs. This is not entirely unsurprising. Removing links randomly from a food-web is
306 effectively the inverse problem of the emergence of a giant component (more than half of the nodes are in
307 a connected network) in random graphs (see Li *et al.* (2021) for a thorough review). The primary
308 difference being that we are removing edges, not adding them, and thus we are witnessing the dissolution
309 of a giant component, rather than the emergence of one. Further applications of percolation theory (Li *et*
310 *al.* 2021) to the topology of sampled ecological networks could improve our understanding of how
311 false-negatives impact the inferences about the structure and dynamics on these networks.

312 Discussion

313 Species interactions enable the persistence and functioning of ecosystems, but our understanding of
314 interactions is limited due to the intrinsic difficulty of sampling them. Here we have provided a null
315 model for the expected number of false-negatives in an interaction dataset. We demonstrated that we
316 expect many false-negatives in species interaction datasets purely due to the intrinsic variation of
317 abundances within a community. We also, for the first time to our knowledge, measured the strength of
318 association between co-occurrence and interactions (Cazelles *et al.* 2016) across many empirical systems,
319 and found that these positive associations are both very common, and showed algebraically that they
320 increase the realized FNR. We have also shown that false-negatives could further impact our ability to
321 both predict interactions and infer properties of the networks, which highlights the need for further
322 research into methods for correcting this bias in existing data.

323 A better understanding of how false-negatives impact species interaction data is a practical
324 necessity—both for inference of network structure and dynamics, but also for prediction of interactions by
325 using species level information. False-negatives could pose a problem for many forms of inference in
326 network ecology. For example, inferring the dynamic stability of a network could be prone to error if the
327 observed network is not sampled “enough.” What exactly “enough” means is then specific to the
328 application, and should be assessed via methods like those here when designing samples. Further,

329 predictions about network rewiring (Thompson & Gonzalez 2017) due to range shifts in response to
330 climate change could be error-prone without accounting for interactions that have not been observed but
331 that still may become climatically infeasible. As is evident from fig. 2(a), we can never guarantee there are
332 no false-negatives in data. In recent years, there has been interest toward explicitly accounting for
333 false-negatives in models (Stock *et al.* 2017; Young *et al.* 2021), and a predictive approach to
334 networks—rather than expecting our samples to fully capture all interactions (Strydom *et al.* 2021). As a
335 result, better models for predicting interactions are needed for interaction networks. This includes
336 explicitly accounting for observation error (Johnson & Larremore 2021)—certain classes of models have
337 been used to reflect hidden states which account for detection error in occupancy modeling (Joseph 2020),
338 and could be integrated in the predictive models of interactions in the future.

339 This work has several practical consequences for the design of surveys for species' interactions.
340 Simulating the process of observation could be a powerful tool for estimating the sampling effort required
341 by a study that takes relative abundance into account, and provides a null baseline for expected FNR. It is
342 necessary to take the size of the species pool into account when deciding how many total samples is
343 sufficient for an “acceptable” FNR (fig. 2(c & d)). Further the spatial and temporal turnover of interactions
344 means any approach to sampling prioritization must be spatiotemporal. We demonstrated earlier that
345 observed negatives outside of the range of both species aren't informative, and therefore using species
346 distribution models could aid in this spatial prioritization of sampling sites.

347 We also should address the impact of false-negatives on the inference of process and causality in
348 community ecology. We demonstrated that in model food webs, false-negatives do not impact the measure
349 of total trophic levels until very high FNR (figure fig. 5(c)), although we cannot generalize this further to
350 other properties. This has immediate practical concern for how we design what taxa to sample—does it
351 matter if the sampled network is fully connected? It has been shown that the stability of subnetworks can
352 be used to infer the stability of the metaweb paper beyond a threshold of samples (Song *et al.* 2022b). But
353 does this extend to other network properties? And how can we be sure we are at the threshold at which we
354 can be confident our sample characterizes the whole system? We suggest that modeling observation error
355 as we have done here can address these questions and aid in the design of samples of species interactions.
356 To try to survey to avoid all false-negatives is a fool's errand. Species ranges overlap to form mosaics,
357 which themselves are often changing in time. Communities and networks don't end in space, and the
358 interactions that connect species on the ‘periphery’ of a given network to species outside the spatial extent

359 of a given sample will inevitably appear as false-negatives in practical samples. The goal should instead be
360 to sample a system enough to have a statistically robust estimate of the current state and empirical change
361 over time of an ecological community at a given spatial extent and temporal resolution, and to determine
362 what the sampling effort required should be prior to sampling.

363 **Acknowledgements**

364 AG & MDC acknowledge the support of the Liber Ero Chair for Biodiversity conservation and NSERC.

365 **References**

- 366 Banville, F., Vissault, S. & Poisot, T. (2021). Mangal.jl and EcologicalNetworks.jl: Two complementary
367 packages for analyzing ecological networks in Julia. *Journal of Open Source Software*, 6, 2721.
- 368 Bascompte, J. & Jordano, P. (2007). Plant-Animal Mutualistic Networks: The Architecture of Biodiversity.
369 *Annual Review of Ecology, Evolution, and Systematics*, 38, 567–593.
- 370 Becker, D.J., Albery, G.F., Sjodin, A.R., Poisot, T., Bergner, L.M., Dallas, T.A., *et al.* (2021). Optimizing
371 predictive models to prioritize viral discovery in zoonotic reservoirs.
- 372 Bezanson, J., Edelman, A., Karpinski, S. & Shah, V.B. (2015). Julia: A Fresh Approach to Numerical
373 Computing.
- 374 Blanchet, F.G., Cazelles, K. & Gravel, D. (2020). Co-occurrence is not evidence of ecological interactions.
375 *Ecology Letters*, 23, 1050–1063.
- 376 Blaom, A.D., Kiraly, F., Lienart, T., Simillides, Y., Arenas, D. & Vollmer, S.J. (2020). MLJ: A Julia package
377 for composable machine learning. *Journal of Open Source Software*, 5, 2704.
- 378 Boakes, E.H., Rout, T.M. & Collen, B. (2015). Inferring species extinction: The use of sighting records.
379 *Methods in Ecology and Evolution*, 6, 678–687.
- 380 Canard, E., Mouquet, N., Marescot, L., Gaston, K.J., Gravel, D. & Mouillot, D. (2012). Emergence of
381 Structural Patterns in Neutral Trophic Networks. *PLOS ONE*, 7, e38295.

382 CaraDonna, P.J., Petry, W.K., Brennan, R.M., Cunningham, J.L., Bronstein, J.L., Waser, N.M., *et al.* (2017).
 383 Interaction rewiring and the rapid turnover of plantpollinator networks. *Ecology Letters*, 20, 385–394.

384 Carlson, C.J., Dallas, T.A., Alexander, L.W., Phelan, A.L. & Phillips, A.J. (2020). What would it take to
 385 describe the global diversity of parasites? *Proceedings of the Royal Society B: Biological Sciences*, 287,
 386 20201841.

387 Cazelles, K., Araújo, M.B., Mouquet, N. & Gravel, D. (2016). A theory for species co-occurrence in
 388 interaction networks. *Theoretical Ecology*, 9, 39–48.

389 Closs, G.P. & Lake, P.S. (1994). Spatial and Temporal Variation in the Structure of an Intermittent-Stream
 390 Food Web. *Ecological Monographs*, 64, 1–21.

391 de Aguiar, M.A.M., Newman, E.A., Pires, M.M., Yeakel, J.D., Boettiger, C., Burkle, L.A., *et al.* (2019).
 392 Revealing biases in the sampling of ecological interaction networks. *PeerJ*, 7, e7566.

393 Gauzens, B., Legendre, S., Lazzaro, X. & Lacroix, G. (2013). Food-web aggregation, methodological and
 394 functional issues. *Oikos*, 122, 1606–1615.

395 Giacomuzzo, E. & Jordán, F. (2021). Food web aggregation: Effects on key positions. *Oikos*, 130,
 396 2170–2181.

397 Griffiths, D. (1998). Sampling effort, regression method, and the shape and slope of sizeabundance
 398 relations. *Journal of Animal Ecology*, 67, 795–804.

399 Gupta, A., Figueroa H., D., O’Gorman, E., Jones, I., Woodward, G. & Petchey, O.L. (2023). How many
 400 predator guts are required to predict trophic interactions? *Food Webs*, 34, e00269.

401 Hadfield, J.D., Krasnov, B.R., Poulin, R. & Nakagawa, S. (2014). A Tale of Two Phylogenies: Comparative
 402 Analyses of Ecological Interactions. *The American Naturalist*, 183, 174–187.

403 Havens, K. (1992). Scale and Structure in Natural Food Webs. *Science*, 257, 1107–1109.

404 Johnson, E.K. & Larremore, D.B. (2021). Bayesian estimation of population size and overlap from random
 405 subsamples.

406 Jordano, P. (2016). Sampling networks of ecological interactions. *Functional Ecology*, 30, 1883–1893.

407 Joseph, M.B. (2020). Neural hierarchical models of ecological populations. *Ecology Letters*, 23, 734–747.

408 Kenall, A., Harold, S. & Foote, C. (2014). An open future for ecological and evolutionary data? *BMC*
409 *Evolutionary Biology*, 14, 66.

410 Khoshraftar, S. & An, A. (2022). A Survey on Graph Representation Learning Methods.

411 Koleff, P., Gaston, K.J. & Lennon, J.J. (2003). Measuring beta diversity for presence-absence data. *Journal*
412 *of Animal Ecology*, 72, 367–382.

413 Kopelke, J.-P., Nyman, T., Cazelles, K., Gravel, D., Vissault, S. & Roslin, T. (2017). Food-web structure of
414 willow-galling sawflies and their natural enemies across Europe. *Ecology*, 98, 1730–1730.

415 Li, M., Liu, R.-R., Lü, L., Hu, M.-B., Xu, S. & Zhang, Y.-C. (2021). Percolation on complex networks:
416 Theory and application. *Physics Reports*, Percolation on complex networks: Theory and application,
417 907, 1–68.

418 MacDonald, A.A.M., Banville, F. & Poisot, T. (2020). Revisiting the Links-Species Scaling Relationship in
419 Food Webs. *Patterns*, 1.

420 Makiola, A., Compson, Z.G., Baird, D.J., Barnes, M.A., Boerlijst, S.P., Bouchez, A., *et al.* (2020). Key
421 Questions for Next-Generation Biomonitoring. *Frontiers in Environmental Science*, 7.

422 Martinez, N.D., Hawkins, B.A., Dawah, H.A. & Feifarek, B.P. (1999). Effects of Sampling Effort on
423 Characterization of Food-Web Structure. *Ecology*, 80, 1044–1055.

424 McLeod, A., Leroux, S.J., Gravel, D., Chu, C., Cirtwill, A.R., Fortin, M.-J., *et al.* (2021). Sampling and
425 asymptotic network properties of spatial multi-trophic networks. *Oikos*, 130, 2250–2259.

426 Moore, A.L. & McCarthy, M.A. (2016). Optimizing ecological survey effort over space and time. *Methods*
427 *in Ecology and Evolution*, 7, 891–899.

428 Niedballa, J., Wilting, A., Sollmann, R., Hofer, H. & Courtiol, A. (2019). Assessing analytical methods for
429 detecting spatiotemporal interactions between species from camera trapping data. *Remote Sensing in*
430 *Ecology and Conservation*, 5, 272–285.

431 Paine, R.T. (1988). Road Maps of Interactions or Grist for Theoretical Development? *Ecology*, 69,
432 1648–1654.

433 Poisot, T. (2022). Guidelines for the prediction of species interactions through binary classification.

434 Poisot, T., Bergeron, G., Cazelles, K., Dallas, T., Gravel, D., MacDonald, A., *et al.* (2021). Global knowledge
 435 gaps in species interaction networks data. *Journal of Biogeography*, 48, 1552–1563.

436 Poisot, T., Ouellet, M.-A., Mollentze, N., Farrell, M.J., Becker, D.J., Brierly, L., *et al.* (2022). Network
 437 embedding unveils the hidden interactions in the mammalian virome.

438 Poisot, T., Stouffer, D.B. & Gravel, D. (2015). Beyond species: Why ecological interaction networks vary
 439 through space and time. *Oikos*, 124, 243–251.

440 Ponisio, L.C., Gaiarsa, M.P. & Kremen, C. (2017). Opportunistic attachment assembles plantpollinator
 441 networks. *Ecology Letters*, 20, 1261–1272.

442 Savage, V.M., Gillooly, J.F., Brown, J.H., West, G.B. & Charnov, E.L. (2004). Effects of Body Size and
 443 Temperature on Population Growth. *The American Naturalist*, 163, 429–441.

444 Song, C., Simmons, B.I., Fortin, M.-J. & Gonzalez, A. (2022a). Generalism drives abundance: A
 445 computational causal discovery approach. *PLOS Computational Biology*, 18, e1010302.

446 Song, C., Simmons, B.I., Fortin, M.-J., Gonzalez, A., Kaiser-Bunbury, C.N. & Saavedra, S. (2022b). Rapid
 447 monitoring for ecological persistence.

448 Stephenson, P. (2020). Technological advances in biodiversity monitoring: Applicability, opportunities
 449 and challenges. *Current Opinion in Environmental Sustainability*, Open issue 2020 part A: Technology
 450 Innovations and Environmental Sustainability in the Anthropocene, 45, 36–41.

451 Stock, M., Poisot, T., Waegeman, W. & De Baets, B. (2017). Linear filtering reveals false negatives in
 452 species interaction data. *Scientific Reports*, 7, 45908.

453 Strydom, T., Catchen, M.D., Banville, F., Caron, D., Dansereau, G., Desjardins-Proulx, P., *et al.* (2021). A
 454 roadmap towards predicting species interaction networks (across space and time). *Philosophical
 455 Transactions of the Royal Society B: Biological Sciences*, 376, 20210063.

456 Thompson, P.L. & Gonzalez, A. (2017). Dispersal governs the reorganization of ecological networks under
 457 environmental change. *Nature Ecology & Evolution*, 1, 1–8.

458 Thompson, R.M. & Townsend, C.R. (2000). Is resolution the solution?: The effect of taxonomic resolution
 459 on the calculated properties of three stream food webs. *Freshwater Biology*, 44, 413–422.

460 Volkov, I., Banavar, J.R., Hubbell, S.P. & Maritan, A. (2003). Neutral theory and relative species abundance
 461 in ecology. *Nature*, 424, 1035–1037.

- 462 Walther, B.A., Cotgreave, P., Price, R.D., Gregory, R.D. & Clayton, D.H. (1995). Sampling Effort and
463 Parasite Species Richness. *Parasitology Today*, 11, 306–310.
- 464 Williams, R.J. & Martinez, N.D. (2000). Simple rules yield complex food webs. *Nature*, 404, 180–183.
- 465 Willott, S.j. (2001). Species accumulation curves and the measure of sampling effort. *Journal of Applied*
466 *Ecology*, 38, 484–486.
- 467 Young, J.-G., Valdovinos, F.S. & Newman, M.E.J. (2021). Reconstruction of plantpollinator networks from
468 observational data. *Nature Communications*, 12, 3911.
- 469 Zhang, S., Tong, H., Xu, J. & Maciejewski, R. (2019). Graph convolutional networks: A comprehensive
470 review. *Computational Social Networks*, 6, 11.